Ultrafast Fiske Effect in Semiconductor Superlattices

Yuriy A. Kosevich,[1,2,*] Anne Beate Hummel,[3] Hartmut G. Roskos,[3,†] and Klaus Köhler[4]
[1]*N. N. Semenov Institute of Chemical Physics, Russian Academy of Sciences, 119991 Moscow, Russia*
[2]*Nanophotonics Technology Center, Polytechnic University of Valencia, E-46022 Valencia, Spain*
[3]*Physikalisches Institut, Johann Wolfgang Goethe-Universität, D-60438 Frankfurt am Main, Germany*
[4]*Fraunhofer-Institut für Angewandte Festkörperphysik, D-79108 Freiburg, Germany*
(Received 23 September 2005; published 6 April 2006)

The current flowing across a semiconductor superlattice in tilted electric and magnetic fields is known to exhibit resonant enhancement, when Landau states of neighboring wells align at certain ratios of the field strengths. We show that the ultrafast version of this effect, in which coherent electron wave packets are involved, has a profound analogy to the Fiske effect in superconductor Josephson junctions and superfluid weak links, in that the coupling of the tunneling-induced charge oscillations (magneto-Bloch versus Josephson oscillations) to another oscillator (in-plane cyclotron oscillations versus external oscillator modes) opens an elastic rectifying transport channel. We explore the superlattice effect both theoretically and experimentally, and find that the transient self-induced current can be adequately modeled if the damping of both types of coupled electron oscillations is properly taken into account.

DOI: 10.1103/PhysRevLett.96.137403 PACS numbers: 78.67.De, 73.21.Cd, 76.40.+b, 78.47.+p

A fundamental property of a quasiparticle in a periodic potential subject to an external force is its localization by Bragg reflection which leads to temporal and spatial oscillations known as Bloch oscillations [1]. They were first observed as oscillations of electronic wave packets in semiconductor superlattices [2–7], and later as a periodic motion of ensembles of ultracold atoms [8,9] and Bose-Einstein condensates [10] in tilted optical lattices.

When subjected to an additional magnetic field, electrons in an electrically biased superlattice experience an effective parabolic potential in addition to that of the periodic lattice, and the additional control parameter gives access to a plethora of physical phenomena.

If the magnetic and electric fields (**B** and **E**) are perpendicular to each other, phase space bifurcates into two clearly separated stable regimes of motion: magneto-Bloch oscillations for dominating electric field, and cyclotronlike oscillations for large magnetic field [11–14]. If, on the other hand, **B** and **E** are nonperpendicular, one finds instead a transition from fairly localized to highly extended electron eigenfunctions for certain ratios of B to E [15–17]. At these so-called Stark-cyclotron resonances, the potential drop per spatial period of the superlattice is an integer multiple of the cyclotron energy allowing coupling of Landau states of neighboring superlattice sites. The ensuing wave function delocalization manifests itself experimentally in an enhanced dc current at the corresponding ratios of B and E [17,18].

The physics associated with this effect is surprisingly rich. It was shown theoretically for the collisionless case that the wave function delocalization could be associated with the existence of chaotic electron orbits [18–20]. But electron wave-packet dephasing in real semiconductor superlattices is by far too rapid to permit experimental access to the multifarious aspects of quantum chaos beyond the enhancement of the incoherent dc current.

Here, we put forth another conceptual aspect of the Stark-cyclotron resonance by considering the profound analogy between electron Bloch oscillations in semiconductor superlattices and the ac Josephson effect in superconductor junctions or superfluid weak links [11,21]. The oscillations are in all cases a consequence of a time-dependent phase difference of the wave functions involved.

Extending this analogy, one can link the existence of the enhanced current in superlattices in a magnetic field to the occurrence of a mode coupling which until now has only been associated with the condensate systems.

This coupling phenomenon, the Fiske effect, is found in superconductor Josephson junctions coupled to electromagnetic resonators [22,23], and in superfluid weak links coupled to mechanical oscillators [24,25]. The Fiske effect manifests itself in a resonant enhancement of the dc charge or mass supercurrent occurring whenever the Josephson frequency matches the frequency of an eigenmode of the resonator or oscillator.

In this Letter, we present both theoretical and direct experimental evidence that resonant mixing between the magneto-Bloch oscillations and the in-plane cyclotron oscillations results in a coherent transient quasi-dc (unidirectional) current and enhanced electric-field screening in a superlattice. The in-plane cyclotron oscillations take on the role which the external resonator or oscillator plays in the case of the condensate systems. The coupling opens an elastic transport channel, which exists only during the coherence time of the electron wave packets involved.

Because of the ultrafast wave-packet dephasing in the superlattice, it is expedient to consider the phenomenon dynamically. Along this line, we first describe time-resolved optical experiments, where we trace the buildup of a pronounced screening field across the superlattice by the resonant transient current which arises after optical excitation of electron and hole wave packets. We then develop the dynamic Fiske-type model and show that it accounts for the observed phenomena.

Figure 1(a) displays the experimental setup. 100-fs pulses (bandwidth: 13 nm) at 1.55 eV from a 82-MHz-repetition-rate Ti:sapphire laser are split in two parts. The more intense ones serve as pump pulses to excite electron-hole pairs. With the delayed weaker pulses, we perform transmittive electro-optic sampling (TEOS) which employs the electro-optic effect in the superlattice itself in combination with differential detection of the p- and s-polarized components of the transmitted light to probe the change of the internal electric field after the decay of an interband-polarization contribution [5,26]. The tensor components of the electro-optic effect are such that the change of the field component in growth direction (x-direction) dominates the signal.

Figure 1(b) shows a sketch of the undoped (100)-oriented superlattice consisting of 35 periods of 9.7-nm-wide GaAs wells and 1.7-nm-wide $Al_{0.3}Ga_{0.7}As$ barriers (width of first electron miniband: 20 meV). The substrate is etched off to allow measurements in transmission. The sample is held at a temperature of 8 K in a split-coil superconducting magnet.

A fixed bias voltage is applied between the n-doped $Al_{0.3}Ga_{0.7}As$ stop-etch layer and a semitransparent Cr/Au Schottky top contact. The resultant internal electric field along the x axis is 10 kV/cm. Under these conditions, the minibands of the field-free superlattice are split into Wannier-Stark states. The wave functions in the conduction band are delocalized while those in the valence band are localized in the individual wells. Spatially overlapping conduction- and valence-band states can be optically coupled by interband transitions, some of which (indexed −1, 0, +1) are indicated in Fig. 1(b).

A magnetic field between 0 and 8 T is applied under an angle of $\Theta = 30°$ relative to the x axis. It induces an additional magnetic quantization, leading to magneto-Wannier-Stark or, synonymously, Stark-cyclotron states.

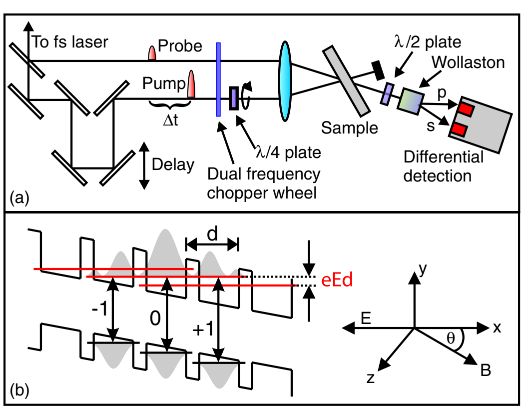

FIG. 1 (color online). (a) Experimental setup; (b) sketch of the electrically biased (100)-oriented superlattice structure. Right side: coordinate systems; the growth direction defines the x direction; Θ is the angle between the electric field in the x direction and the magnetic field in the x-z plane.

Electron wave packets are produced via simultaneous excitation of several of the spatially overlapping conduction-band states by the light pulses, initiating a quantum interference of these states [2–7,13]. The ensuing electric-field dynamics is traced by TEOS. Figure 2 displays measured signals as a function of the delay time between pump and probe pulses at fixed bias field and for a magnetic field varied from 0 to 8 T in steps of 0.2 T. Each transient consists of an oscillatory contribution on a shifting background. As the electro-optic effect predominantly addresses electric dipole moments in x direction, only the magneto-Bloch oscillations are visible, not the in-plane cyclotron oscillations.

We focus on the shifting background signal which reflects the buildup of the screening field. Figure 3(a) shows the measured data in a three-dimensional parameter space. One can discern the oscillatory signals, but most striking is the reduction of the signal at later delay times at magnetic fields around 6 T, where the magneto-Bloch oscillations and the in-plane cyclotron oscillations are expected to be at resonance (see below). The signal reduction is attributed to enhanced field screening indicating the existence of a resonant quasi-dc Stark-cyclotron (or Fiske) current.

In order to theoretically address these phenomena, we work in the semiclassical picture which is known to adequately describe quantum coherence phenomena because a macroscopically large number of carriers contributes to the coherent response [11,12]. We consider the coupling of the electron velocity along the x direction, $V_x = v_x^{\max} \times \exp(-\gamma_B t)\sin(p_x d/\hbar)$, with the transverse (Hall) velocity V_y. Here, $v_x^{\max} = \hbar/(m_x d)$ is the maximal miniband group velocity [$m_x = 0.115 m_e$ [13]], d denotes the superlattice period, p_x the Bloch momentum, and $\gamma_B = 1/\tau_B$ the relaxation rate of the magneto-Bloch oscillations. The interaction with V_y occurs via both phase and amplitude of the

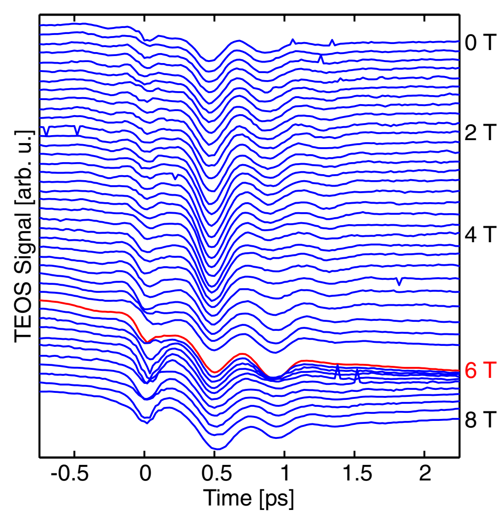

FIG. 2 (color online). TEOS transients for fixed electric and varied magnetic fields (0–8 T in steps of 0.2 T). $t = 0$ ps: arrival of pump. At 6 T, the magneto-Bloch oscillations and the in-plane cyclotron oscillations (not visible) are at resonance ($\omega_B = \omega_{cx}$).

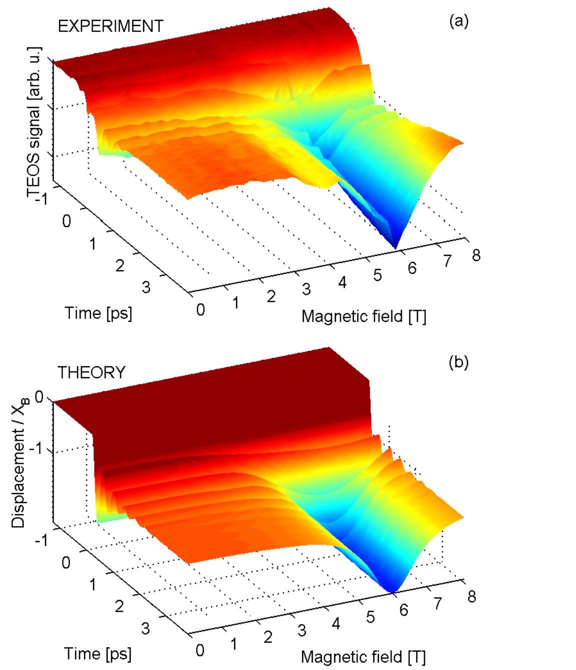

FIG. 3 (color online). Comparison between experiment and theory. (a) TEOS signals of Fig. 2 highlighting the slowly varying background signal. (b) Numerically calculated displacement $-X(t)/X_B$ of coherent electrons in units of the amplitude of the magneto-Bloch oscillations for $\omega_B\tau_B = 8.1$, $\tau_B = 0.6$ ps, and $\tau_c = 10\tau_B$.

magneto-Bloch oscillations [27]:

$$\dot{p}_x = e(E_x + B_z V_y), \quad (1)$$

$$\ddot{V}_y + 2\gamma_c \dot{V}_y + (\omega_{cx}^2 + \gamma_c^2)V_y = -\omega_{cz}(\dot{V}_x + \gamma_c V_x), \quad (2)$$

where $\gamma_c = 1/\tau_c$ is the relaxation rate of the in-plane cyclotron oscillations, and $\omega_{cx,z} = eB_{x,z}/m^*$ denote the cyclotron frequencies ($m^* = 0.067m_e$).

The coupling of the two types of motion results in the change of the electron velocity V_x through its phase:

$$V_x = v_x^{\max}\exp(-\gamma_B t)\sin\Big\{\omega_B t - C\Big[\exp(-\gamma_B t) \times \sin(\omega_B t + \Phi) - \frac{\omega_B \exp(-\gamma_c t)}{\omega_{cx}}\sin(\omega_{cx} t + \Phi) - \Big(1 - \frac{\omega_B}{\omega_{cx}}\Big)\sin\Phi\Big]\Big\}, \quad (3)$$

$$C = \frac{m^*}{m_x}\frac{\tan^2\Theta\,\omega_{cx}^2}{\sqrt{(\omega_{cx}^2 - \omega_B^2)^2 + 4\omega_B^2(\gamma_B - \gamma_c)^2}},$$

$$\Phi = \arccos\Big[\frac{\omega_{cx}^2 - \omega_B^2}{\sqrt{(\omega_{cx}^2 - \omega_B^2)^2 + 4\omega_B^2(\gamma_B - \gamma_c)^2}}\Big].$$

Equation (3) has been derived for the initial conditions $p_x(0) = 0$, $V_x(0) = 0$, and $V_y(0) = 0$, realized in the experiment, and is valid for $\omega_B \gg \gamma_B$ and $\omega_{cx} \gg \gamma_c$. It describes, in addition to magneto-Bloch oscillations with the angular frequency $\omega_B = (eE_x d)/\hbar$, a unidirectional drift of the electrons in x direction. The latter component of the coherent electron velocity is most pronounced when the magneto-Bloch oscillations and the in-plane cyclotron oscillations are in resonance. For this case, $\omega_B = \omega_{cx}$, one derives from Eq. (3) the following time dependence of the transient quasi-dc component of the velocity:

$$V_{x,\mathrm{res}}^{\mathrm{qdc}}(t) = v_x^{\max}\exp(-\gamma_B t) \times J_1[C_r|\exp(-\gamma_c t) - \exp(-\gamma_B t)|], \quad (4)$$

where $C_r = \omega_B \tan^2\Theta(m^*/2m_x)/\mid\gamma_B - \gamma_c\mid$ is the resonance coupling parameter and $J_1(x)$ is the Bessel function of first order. In the limit of $\gamma_B = 0$, finite γ_c and $t \gg \tau_c$, $V_{x,\mathrm{res}}^{\mathrm{qdc}}$ transforms into a constant velocity $V_{x,\mathrm{res}}^{\mathrm{dc}} = v_x^{\max}J_1[\omega_B\tau_c\tan^2\Theta(m^*/2m_x)]$ and results in a self-induced dc current fully analogous to that of the Fiske effect in Josephson junctions. For finite γ_B and γ_c, $V_{x,\mathrm{res}}^{\mathrm{qdc}}$ gives rise to the transient equivalent of the Fiske current.

The quantity measured in the experiment is the time-dependent internal depolarization field $E_x^{\mathrm{dep}}(t) = -4\pi e N^{\mathrm{coh}}X(t)/\epsilon_\infty$, where $X(t)$ is the time-dependent average electron-hole separation $[X(t) = \int_0^t V_x(t')dt'$, see Eq. (3)], which here is identical to the electron displacement because the optically excited heavy holes do not perform magneto-Bloch oscillations and remain at the point of excitation during the relevant time scale; N^{coh} denotes the density of photo-excited coherent electrons; $\epsilon_\infty = 13$ is a background dielectric constant.

Figure 3(b) plots the normalized displacement $-X(t)/X_B$ numerically calculated with the help of Eq. (3), $X_B = v_x^{\max}/\omega_B$ being the spatial amplitude of the magneto-Bloch oscillations, for $\omega_B = 2\pi \times 2.16$ THz, $\Theta = 30°$, and assuming $\omega_B\tau_B = 8.1$ and $\tau_c = 10\tau_B$, which is based on the fit to the data of Fig. 3(a) for large delay times (see Fig. 4 below), yielding $\tau_B \approx 0.6$ ps and $\tau_c \approx 6$ ps [see also [13] and cf. $\tau_c \approx 5$ ps for optically excited bulk GaAs [28]]. With these parameters, we find that $C_r \approx 0.8$ in our system.

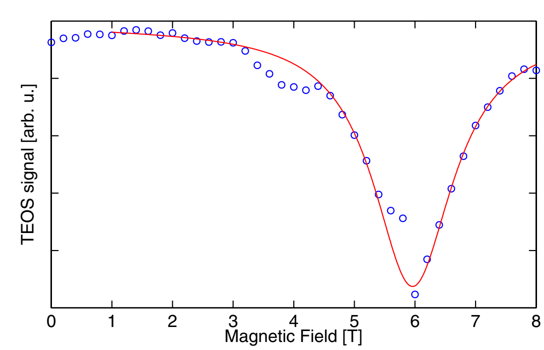

FIG. 4 (color online). Enhanced field screening at late delay times. Dots: TEOS signals vs B, averaged for $t = 1.7$–3.8 ps (the coherent oscillations have almost died out after $t = 1.7$ ps). Full line: fit according to Eq. (5), which gives $\tau_c \approx 6$ ps and $\tau_B \approx 0.6$ ps. The latter is close to the value of $\tau_B \approx 0.5$–0.6 ps, given by the independent fit to the data of Fig. 2 for low magnetic fields. This indicates the consistency of the model.

The agreement with the experimental curves is striking. The simulations reproduce the enhanced field screening, thus confirming it as being of coherent nature.

The enhanced screening for large delay times is proportional to the resonant displacement enhancement $\Delta X^{(\infty)}$, which is obtained as the time integral of Eq. (3) minus that far off the resonance (the latter time integral yielding the value X_B). In the case of $C_r < 1$, valid here, $\Delta X^{(\infty)}$ has the following form:

$$\Delta X^{(\infty)} = A\bigg\{2\omega_B(\gamma_c - \gamma_B) \times \bigg[\frac{1}{2\gamma_B\omega_B} - \frac{\gamma_B + \gamma_c}{\omega_{cx}[(\omega_{cx} - \omega_B)^2 + (\gamma_B + \gamma_c)^2]}\bigg] + \frac{(\omega_{cx} - \omega_B)^2(\omega_{cx} + \omega_B)}{\omega_{cx}[(\omega_{cx} - \omega_B)^2 + (\gamma_B + \gamma_c)^2]}\bigg\},$$
$$A = v_x^{\max}\frac{m^*}{2m_x}\frac{\tan^2\Theta\,\omega_B\omega_{cx}^2}{(\omega_{cx}^2 - \omega_B^2)^2 + 4\omega_B^2(\gamma_B - \gamma_c)^2}. \quad (5)$$

Figure 4 demonstrates that the magnetic-field dependence of the TEOS signal at late delay times indeed has the near-Lorentzian line shape predicted by Eq. (5). The width of the curve along the magnetic-field axis is given approximately by the sum of the Bloch and cyclotron damping rates. The displacement enhancement at resonance, $\Delta X_{\rm res}^{(\infty)} = v_x^{\max}\tan^2\Theta(m^*/8m_x)\omega_B\tau_B^2\tau_c/(\tau_B + \tau_c)$ for $C_r < 1$, is determined, in contrast, by the shorter of the two relaxation times, equal to τ_B in our system. As follows from Eq. (4), $\Delta X_{\rm res}^{(\infty)}$ remains finite (i.e., the Wannier-Stark localization persists) in the collisionless limit $(\gamma_B, \gamma_c) \to 0$. For relatively low scattering rates $(\gamma_B, \gamma_c) \ll \omega_B$, $\Delta X^{(\infty)}\gamma_B$ determines the enhancement of the incoherent steady-state electron velocity along the superlattice axis as a function of the **E** and **B** fields [12].

It is also worth mentioning that the coupling between the magneto-Bloch and in-plane cyclotron oscillations in tilted **E** and **B** fields does not considerably change the Bloch-oscillation frequency, in contrast to the case of perpendicular fields. The reason is that in the latter case the Bloch frequency is significantly influenced by the quasi-dc coherent Hall velocity [11,13], while the Hall velocity becomes oscillatory due to the in-plane cyclotron oscillations in tilted fields [for $\omega_{cx} \gg \gamma_c$, see Eq. (2)] and the change of the Bloch frequency is strongly suppressed (averaged out) by Hall velocity oscillations [27]. Figure 2 corroborates this finding experimentally.

In conclusion, we show the appearance of a self-induced quasi-dc current in an optically excited semiconductor superlattice in tilted electric and magnetic fields. The current is substantially enhanced at the resonance between the magneto-Bloch and in-plane cyclotron oscillations. The effect has a profound analogy to the Fiske effect in superconductor Josephson junctions and superfluid weak links. The self-induced current in the semiconductor superlattice is, however, transient and for its adequate modeling, the damping of both types of coupled electron oscillations must be taken into account. Similar transient self-induced current, caused by nonresonant coupling of damped Bloch oscillations to *coherent plasmons* [7,11], can be the origin of the coherent quasi-dc current, observed in a biased semiconductor superlattice [29].

Funding by the Deutsche Forschungsgemeinschaft, discussions with E. Mohler, A. Buchleitner, S. Flach, A. Kolovsky, and Yu. Proshin, and the hospitality of the MPI PKS, Dresden, where Yu. A. K. performed part of this work, are gratefully acknowledged.

*Electronic address: yukosevich@yahoo.com
†Electronic address: roskos@physik.uni-frankfurt.de

[1] L. Esaki and R. Tsu, IBM J. Res. Dev. **14**, 61 (1970).
[2] J. Feldmann *et al.*, Phys. Rev. B **46**, R7252 (1992).
[3] K. Leo *et al.*, Solid State Commun. **84**, 943 (1992).
[4] C. Waschke *et al.*, Phys. Rev. Lett. **70**, 3319 (1993).
[5] T. Dekorsy, P. Leisching, K. Köhler, and H. Kurz, Phys. Rev. B **50**, R8106 (1994).
[6] R. Martini *et al.*, Phys. Rev. B **54**, R14325 (1996).
[7] F. Löser, Yu. A. Kosevich, K. Köhler, and K. Leo, Phys. Rev. B **61**, R13373 (2000).
[8] M. BenDahan *et al.*, Phys. Rev. Lett. **76**, 4508 (1996).
[9] S.R. Wilkinson *et al.*, Phys. Rev. Lett. **76**, 4512 (1996).
[10] B.P. Anderson and M.A. Kasevich, Science **282**, 1686 (1998).
[11] Yu. A. Kosevich, Phys. Rev. B **63**, 205313 (2001).
[12] Yu. A. Kosevich, Phys. Rev. Lett. **88**, 229701 (2002).
[13] T. Bauer *et al.*, Phys. Rev. Lett. **88**, 086801 (2002).
[14] A.B. Hummel *et al.*, Phys. Status Solidi B **242**, 1175 (2005).
[15] F.G. Bass, V.V. Zorchenko, and V.I. Shashora, Pis'ma Zh. Eksp. Teor. Fiz. **31**, 345 (1980) [JETP Lett. **31**, 314 (1980)].
[16] F.G. Bass and V.M. Polyanovskii, Fiz. Tekh. Poluprovodn. **21**, 1207 (1987) [Sov. Phys. Semicond. **21**, 733 (1987)].
[17] L. Canali, M. Lazzarino, L. Sorba, and F. Beltram, Phys. Rev. Lett. **76**, 3618 (1996).
[18] T.M. Fromhold *et al.*, Nature (London) **428**, 726 (2004).
[19] T.M. Fromhold *et al.*, Phys. Rev. Lett. **87**, 046803 (2001).
[20] S.P. Stapleton *et al.*, Physica (Amsterdam) **199D**, 166 (2004).
[21] A. A. Ignatov, K. F. Renk, and E. P. Dodin, Phys. Rev. Lett. **70**, 1996 (1993).
[22] M. Tinkham, *Introduction to Superconductivity* (McGraw-Hill, New York, 1996).
[23] K.K. Likharev, *Dynamics of Josephson Junctions and Circuits* (Gordon and Breach, New York, 1986).
[24] R.W. Simmonds *et al.*, Phys. Rev. Lett. **81**, 1247 (1998).
[25] J.C. Davis and R.E. Packard, Rev. Mod. Phys. **74**, 741 (2002).
[26] R. Lövenich *et al.*, Solid State Commun. **101**, 167 (1997).
[27] Yu. A. Kosevich, Phys. Stat. Sol. C **0**, 1467 (2003).
[28] D. Some and A.V. Nurmikko, Phys. Rev. B **50**, R5783 (1994).
[29] F. Löser *et al.*, Phys. Rev. Lett. **85**, 4763 (2000).